OXFORD

Journal of Geophysics and Engineering

Journal of Geophysics and Engineering (2024) **21**, 413–425

https://doi.org/10.1093/jge/gxae012

Advance access publication 27 January 2024

Mapping of geological structures and sediment thickness from analysis of aeromagnetic data over the Obudu Basement Complex of Nigeria

Stephen E. Ekwok[1], Ahmed M. Eldosuoky[2,3,*], Edward A. Thompson[1], Romeo A. Ojong[4], Anthony M. George[1], Saad S. Alarifi[4], Sherif Kharbish[2,3], Peter András[5] and Anthony E. Akpan[1]

[1] Geophysics Unit, Department of Physics, University of Calabar, P.M.1115, Calabar, Cross River State, Nigeria
[2] Geology Department, Faculty of Science, Suez University, Suez, 43518, Egypt
[3] Academy of Scientific Research & Technology, Cairo, Egypt
[4] Department of Geology, University of Calabar, P.M.1115, Calabar, Cross River State
[5] Department of Geology and Geophysics, College of Science, King Saud University, P.O. Box 2455, Riyadh 11451, Saudi Arabia
[6] Faculty of Natural Sciences, Matej Bel University in Banska Bystrica, Tajovského 40, 974 01 Banska Bystrica, Slovakia

*Corresponding authors. E-mail: dr_a.eldosoky@yahoo.com; E-mail: Ahmed.Eldosouky@sci.suezuni.edu.eg

Received: August 19, 2023. **Revised:** December 4, 2023. **Accepted:** January 26, 2024

Abstract

In this study, geologic structures, as well as attendant orientations and sediment thickness, in the Nigerian Obudu Complex were delineated using the Centre for Exploration Targeting (CET), and depth determination methods such as source parameter imaging (SPI) and standard Euler deconvolution (SED). The CET, SPI, and SED procedures were applied on the total magnetic intensity data. Also, the enhanced TMI data using analytic signal, first-vertical derivative, total-horizontal derivative, and tilt-angle derivative filters were further subjected to CET operation, with the aim of mapping both subtle and prominent lineaments. In general, mapped geologic structures trends in the NE–SW, NNE–SSW, E–W, and N–S directions. Overall, the dominant geologic structural orientations of NE–SW and NNE–SSW reflect the regional strike orientation. The regional striking of the lineation, which is caused by the Pan-African orogeny and subsequent post-orogenic processes, has an impact on these orientations. The N–S and E–W structural deviations from the main NE–SW and NNE–SSW trends are initiated by the YGS of the post-orogenic events. Overall, these complex geologic structures are probable sites for metallogenic minerals.

Keywords: Centre for Exploration Targeting; geologic structures; Obudu Basement rock; source parameter imaging; standard Euler deconvolution

1. Introduction

Precise mapping of geologic structures plays a pivotal role in the Earth sciences (Eldosouky *et al.* 2022a, Ekwok *et al.* 2023a, 2023b). Understanding the distribution and geometry of subsurface features, such as folds, faults, fractures, and intrusive rocks, is essential for deciphering tectonic processes, assessing mineral potential, and locating hydrocarbon reservoirs (Smith *et al.* 2018a; Kusky 2020, Elkhateeb *et al.* 2021, Pham *et al.* 2021a, 2021b, Eldosouky *et al.* 2022a, 2022b). Over the years, numerous methods have been employed to delineate these structures, utilizing a range of geological and geophysical techniques (Abdelrahman

et al., 2023a; Eldosouky *et al.* 2022b, 2022c; GSC 1992). Traditional approaches to mapping subsurface structures have relied on field observations, borehole data, and seismic surveys (Richter 2017, Tselentis *et al.* 2020). While these methods have proven effective, they are often associated with limitations in terms of cost, accessibility, and resolution capabilities (Tselentis *et al.* 2020, Ben *et al.* 2022a, 2022b).

In recent decades, magnetic data have emerged as a valuable and cost-effective tool for investigating geologic structures due to the wide availability, non-invasive nature, and sensitivity to magnetic anomalies associated with various subsurface features (Blakely 1996, Alfaifi *et al.* 2023). For the purpose of outlining lineation using potential field techniques, some enhancement filters have recently been developed (Ekwok *et al.* 2022a, 2022b). The two filters that are most frequently employed for geologic structural studies are the analytic signal (ASIG) and total-horizontal derivative (THD) (Eldosouky *et al.* 2022b). These filters produce somewhat diffuse lineament maps, however, they are frequently used to qualitatively assess magnetic data (Prasad *et al.* 2022). Nonetheless, in an attempt to overcome the setbacks of conventional edge-detection techniques, numerous alternative enhancement filters focused on potential field gradients have been developed (Eldosouky *et al.* 2022b). The tilt-derivative technique was developed by Fedi and Florio (2001) and is centred on the arctan function of the vertical gradient to THD ratio (Miller and Singh 1994), the tilt-derivative of gradient amplitude, and the THD obtained by averaging the vertical gradients. While Cooper and Cowan (2006) established the normalized gradient-amplitude approach, other scholars such as Wijns *et al.* (2005) produced the theta-method, which employs the gradient amplitude to normalize the overall gradient. Other enhancement filters for edge detection that depend on magnetic and gravity data are well documented by Salem *et al.* (2007), plus the ones already described.

On the whole, the ASIG is a mathematical transformation that offers a measure of the amplitude of the magnetic anomaly and its phase (Nabighian 1972). This filtering technique is useful for mapping the boundaries of magnetic sources, such as faults and geological contacts (Nabighian 1972). The TDR calculates the gradient of the potential field data, emphasizing the steepness of the magnetic or gravity gradient (Nabighian 1972). It helps in delineating structural features and is mainly useful for identifying the boundaries of subsurface geological bodies, which are often associated with geologic structures like faults, dykes, and mineral deposits (Nabighian 1972). The THD is another geophysical filtering technique that calculates the gradient only along the horizontal directions, neglecting the vertical component of the data (Roest *et al.* 1992). This filtering approach highlights lateral changes in the magnetic or gravity data and can help in mapping structures that are predominantly horizontal or sub-horizontal in nature (Roest *et al.* 1992). However, the FVD is a gradient filtering technique that highlights vertical changes in the magnetic or gravity data (Nabighian *et al.* 2005). Unlike the THD, it emphasizes the vertical component of potential field anomalies. The FVD is particularly useful for identifying near-surface structures and can aid in mapping shallow geological features (Nabighian *et al.* 2005).

Furthermore, an improved and very precise filter such as the CET can accurately map lineaments originating from vertical and horizontal magnetic anomalies (Kovesi 1991, 1997, Lam *et al.* 1992, Holden *et al.* 2008, 2010). The CET employs advanced modelling techniques and geospatial analysis to identify areas with high mineral potential (Holden *et al.* 2008). It aims to provide a holistic understanding of geological processes and mineralization patterns to guide exploration efforts more effectively (Holden *et al.* 2010). According to Grose *et al.* (2017), the CET has recently been at the forefront of research into fresh and inventive methods for defining geologic structures using airborne potential field data. The method has gained prominence for its cutting-edge research in the realm of exploration and resource targeting (Heal *et al.* 2014, Grose *et al.* 2017). While initially developed for mineral exploration (Jessell *et al.* 2016), the CET applicability extends to mapping geologic structures with remarkable accuracy (Smith *et al.* 2019). It can be applied to diverse geophysical data sets, such as seismic, magnetic, or gravity data, to derive a holistic understanding of subsurface structures (Dentith and Mudge 2014, Smith *et al.* 2019). The application of this improved technique allows for a comprehensive understanding of subsurface geological structures, precise mapping, and interpretation (Heal *et al.* 2014), as well as identification of subtle structural features that contribute to a better understanding of the geological history of an area (GSC 1992, Jessell *et al.* 2016). Recent studies have demonstrated the efficacy of the CET method in analysing and interpreting aeromagnetic data (Uwiduhaye *et al.* 2021, Ekwok *et al.* 2022a).

Assessment of the position and depth of geologic anomalies is one of the main uses of aeromagnetic data (Ekwok *et al.* 2021). Traditionally, magnetic data have been utilized in locating the depth to geologic structures for mineral exploration. By integrating two or more depth estimation techniques (Salem and Ravat 2003), or by improving the signal-to-noise ratio through the evaluation of derivatives of the field (Davis and Li 2009), the issue of erroneous solutions in depth estimation using various depth determination procedures can be solved. According to Smith *et al.* (1998), the SPI and SED methods are not dependent on any geologic model assumptions. As a result, the use of these methods has greatly simplified the process of interpreting magnetic data (Smith *et al.* 1998).

This research offers a wide-ranging analysis of the application of CET on TMI, and enhanced magnetic data subjected

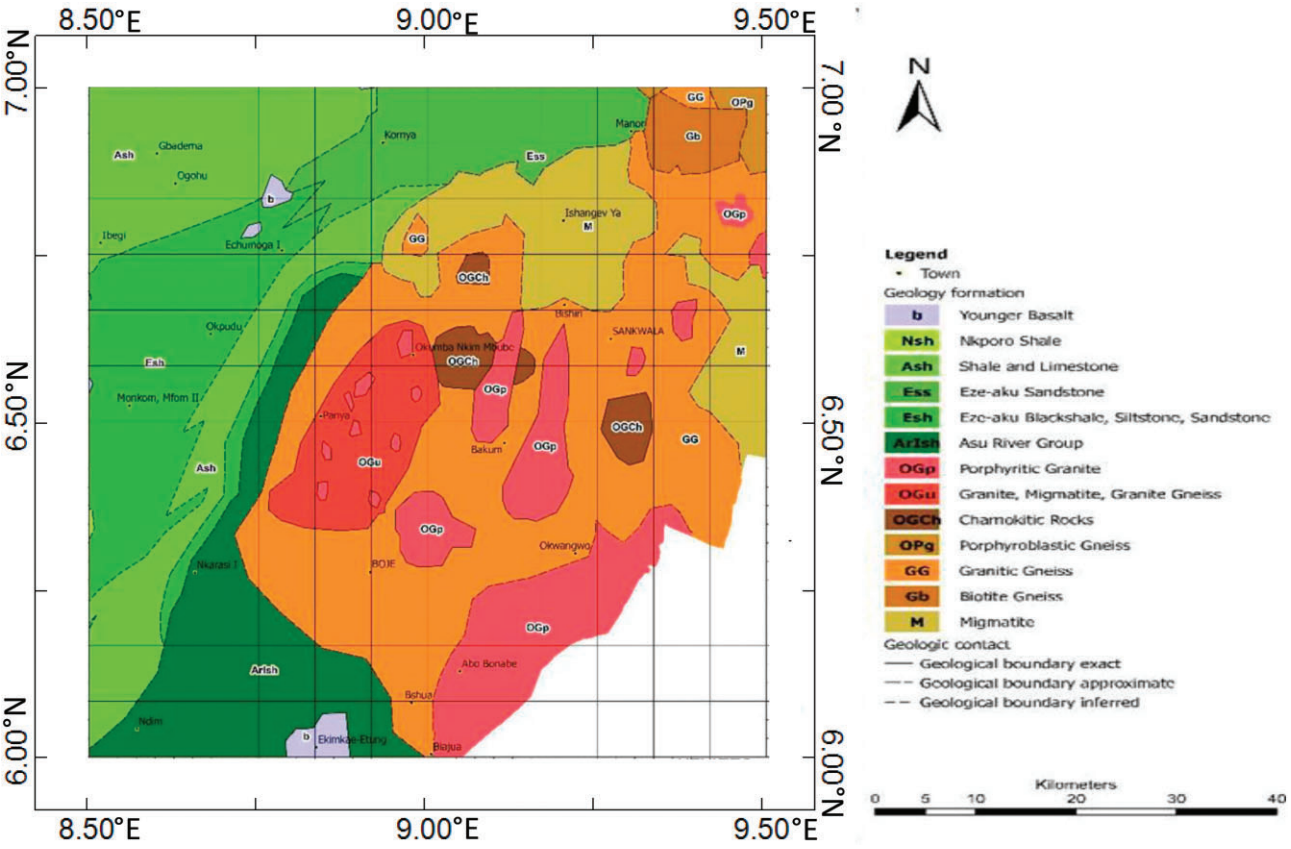

Figure 1. Geologic map of the study area.

to FVD, ASIG, THD, and TDR filters. Furthermore, the SPI (Thurston and Smith 1997) and SED (Reid *et al.* 1990), were applied on the reduced TMI data. The application of these advanced techniques on the aeromagnetic data resulted to the identification and interpretation of lineaments, as well as the generation of depth solution maps, which proved useful for mineral exploration targeting in the Obudu Basement Complex of Nigeria. A significant advancement in the analysis involves the interpretation of structural maps in conjunction with geological information of the study location (Roest *et al.* 1992, Nabighian *et al.* 2005, Thompson *et al.* 2019, Kusky 2020). The structural complexity maps are expected to identify zones of metallogenic minerals connected to hydrothermal modifications and structural control triggered by intrusives (Ekwok *et al.* 2022a).

2. Location, geology, and tectonics of the Obudu Basement

The Obudu Basement rocks of southeastern Nigeria encompass a significant geological formation that provides valuable insights into the region's geological history (Asouzu and Onyeagocha 2013, Obiora *et al.* 2016). Geographically, the investigated region, which is positioned in the southeastern part of Nigeria, is dominated by an extensive outcrop of ancient crystalline rocks that form the basement of the sedimentary Benue Trough (Nwankwo 2009). This area is sited approximately between longitudes 8° 30′–9° 30′ E and latitudes 6°30′–7°00′ N (Fig. 1).

According to geological studies, the rocks that make up the Obudu Basement are made up of a wide variety of rock types, including granite, gneiss, schist, amphibolite, and migmatite (Ajibade *et al.* 2010, Asouzu and Onyeagocha 2013, Obiora *et al.* 2016). These rocks, which belong to the Nigerian Precambrian Basement Complex, constitute the oldest (Asouzu and Onyeagocha 2013). These deformations have produced a variety of structural features, such as folds, faults, and shear zones, which have influenced the present-day geometry of the rocks (Ajibade *et al.* 2010, Asouzu and Onyeagocha 2013). According to Obiora *et al.* (2016), these fault systems resulted to a substantial impact on the tectonic evolution and structural development of the basement rocks.

The Basement Complex is further classified into two main units: the OGS and the YGS (Nwankwo 2009, Ajibade *et al.* 2010, Asouzu and Onyeagocha 2013, Obiora *et al.* 2016).

The Older Granite Suite within the Obudu Basement rocks is predominantly composed of medium- to coarse-grained biotite and muscovite granites (Nwankwo 2009, Asouzu and Onyeagocha 2013, Obiora *et al.* 2016). These granites exhibit a variety of textures, ranging from porphyritic

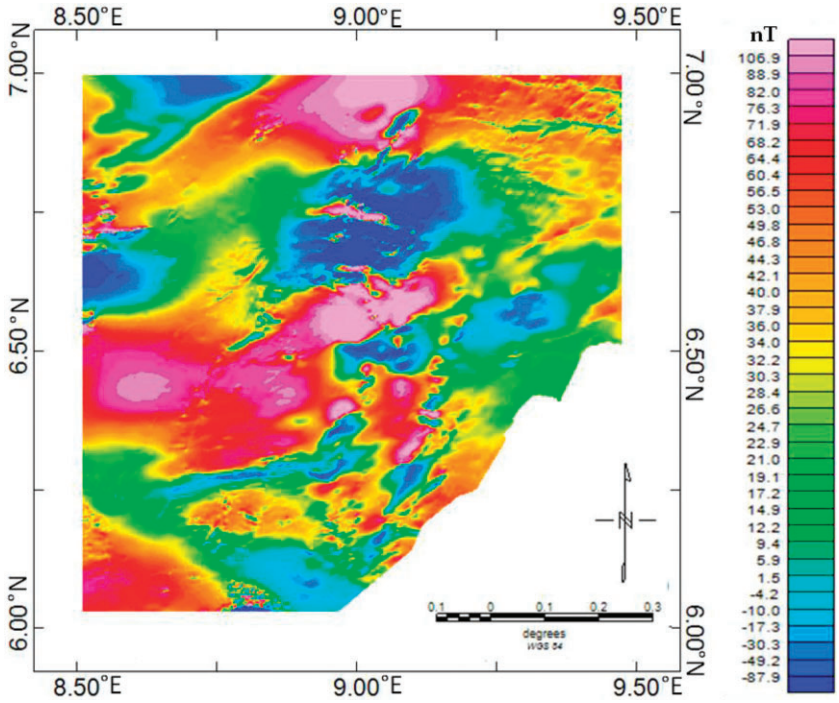

Figure 2. Total magnetic intensity map.

to equigranular (Asouzu and Onyeagocha 2013, Obiora *et al.* 2016). The YGS, on the other hand, comprises fine- to medium-grained biotite and muscovite granites, as well as granodiorites and syenites. These granites often display distinctive porphyritic textures (Asouzu and Onyeagocha 2013, Obiora *et al.* 2016).

Tectonically, the Obudu Basement rocks have undergone complex deformation processes throughout their geological history (Asouzu and Onyeagocha 2013, Obiora *et al.* 2016). A number of tectonic events, including the Pan-African orogeny and later post-orogenic activity, have had an impact on the area (Ajibade *et al.* 2010). The Pan-African orogeny, which occurred around 600–500 million years ago, led to the formation of mountain belts and the amalgamation of different continental blocks in West Africa (Nwankwo 2009).

The Obudu Basement rocks have witnessed severe tectonism throughout the Pan-African orogeny, resulting in folding, faulting, and metamorphism (Nwankwo 2009). The rocks exhibit a polyphase deformation history, reflecting multiple episodes of tectonic activity.

3. Data collection and methodology

The airborne magnetic data used in this study to map the structural complexity of the Precambrian Obudu Basement Complex were collected by Fugro Airborne Services, Canada, from 2005 to 2010. The data were measured using a flux-adjusting surface data assimilation system with a flight-line spacing of 100 m, tie line spacing of 500 m, and terrain clearance of between 80 and 100 m along 826 000 lines. The flight-line direction was basically NW–SE whereas the tie lines, which were intended to traverse the leading geological strike bearing, were oriented mainly NE–SW. The measured data were filtered, and all the required reductions were carried out by Fugro Airborne Services, Canada, before been submitted in gridded and digitized format to the Nigerian Geological Survey Agency (NGSA). These modern data (Fig. 2) obtained from NGSA at subsidized rate were observed to be suitable for hydrocarbon and mineral explorations as well as mapping of geological structures.

In this investigation, standard magnetic data enhancement techniques such as the ASIG, FVD, THD, and TDR were applied (Fig. 3). The gridded results from these filter procedures were further enhanced using the CET. The magnetic dataset is enhanced using filtering procedures that carefully magnify the anomalies from geological sources (Milligan and Gunn 1997).

Computing the FVD during magnetic investigation has similar advantages to directly detecting the vertical gradient with a magnetic gradiometer, including enhancing shallow magnetic bodies and improving the resolution of the sources (Pal and Majumdar 2015). The *n*th derivative is expression as

$$F(\omega) = \omega^n, \tag{1}$$

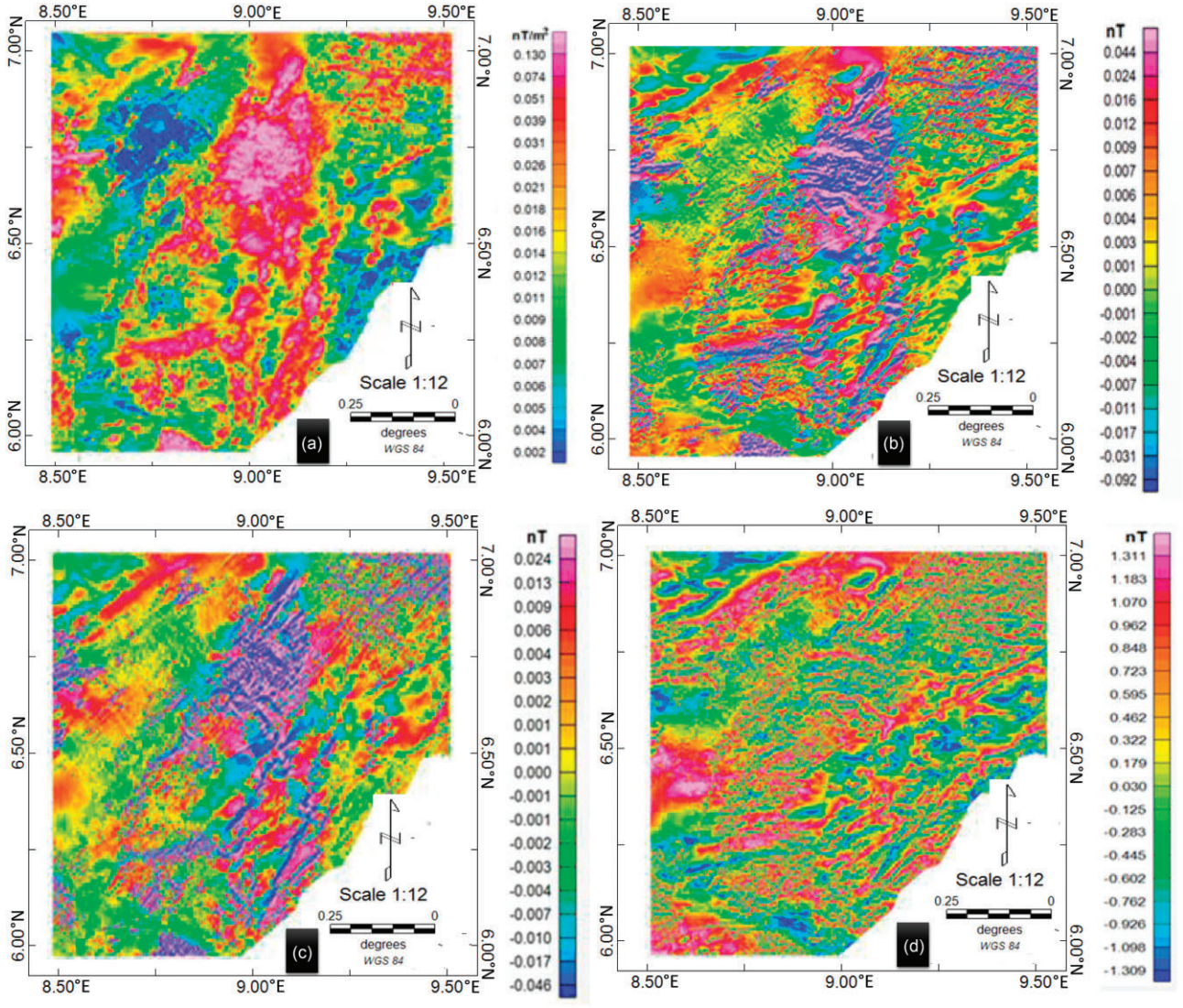

Figure 3. (a) ASIG, (b) first-vertical derivative, (c) THD, and (d) tilt-angle derivative maps.

The THD, which is defined as follows, is an extensively applied edge-detection filter (Blakely 1996):

$$THD_{(x,y)} = \left[\left(\frac{\partial A}{\partial x}\right)^2 + \left(\frac{\partial A}{\partial y}\right)^2\right]^{\frac{1}{2}}, \qquad (2)$$

where $\frac{\partial T}{\partial x}$ and $\frac{\partial T}{\partial y}$ are the two orthogonal horizontal derivatives of the magnetic data, and the magnetic anomaly is A.

The ASIG produces maximum responses over magnetic sources (Nabighian 1972, 1984). As a result of the typical difficulty commonly associated with the reduction-to-pole operation, this method is often utilized at low magnetic latitudes. Roest *et al.* (1992) used the three orthogonal derivatives of the magnetic data to determine the amplitude of the ASIG:

$$\left|ASIG_{(x,y)}\right| = \sqrt{\left(\frac{\partial A}{\partial x}\right)^2 + \left(\frac{\partial A}{\partial y}\right)^2 + \left(\frac{\partial A}{\partial z}\right)^2}, \qquad (3)$$

the measured magnetic data defined by A in Equation (3).

The TDR is less sensitive to noise than other enhancement techniques that use higher order derivatives. It serves as a marker for the boundaries of geologic features that contribute to magnetic anomalies. The TDR is described as the anomalies' vertical derivative divided by their horizontal derivative. The formula is as follows:

$$\theta = \tan^{-1} = \frac{\frac{\partial^2 A}{\partial z^2}}{THD_{(x,y)}}. \qquad (4)$$

The steps involved in CET analysis include structural complexity, lineation detection, texture analysis, and lineation vectorization procedures. These programs can be used for a variety of tasks, including grid texture analysis, edge detection, thresholding, lineament recognition, and locating structurally complicated regions (Kovesi 1991, 1997, Lam

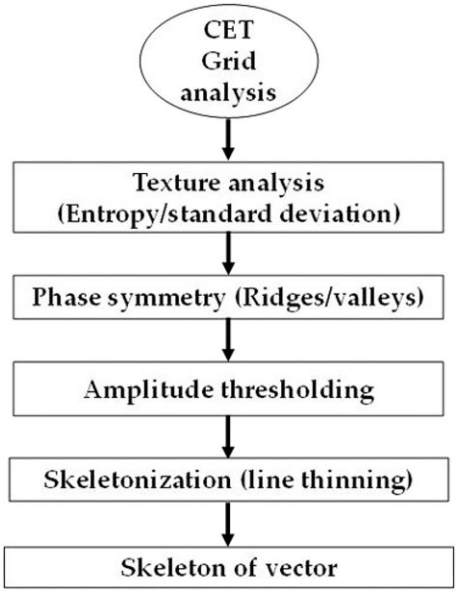

Figure 4. The flow chart of the CET algorithm applied to magnetic data.

et al. 1992) (Fig. 4). The detailed trend detection menu is designed specifically for the detection of discontinuities in magnetic and gravity data. Entropy and standard deviation are two distinct methods (i.e. ridges and edges in the texture) for estimating trends that are included in this menu (Kovesi 1991, 1997, Lam *et al.* 1992).

Within localized windows of a dataset, the entropy plugin offers a measurement of the textural information. It quantifies the data into discrete bins to determine the total number of discrete values that resulted from that quantization (Holden *et al.* 2008, 2010). This analysis is used to determine the statistical unpredictability of neighbourhood data values. Assigned a definite number of bins, n, for a particular cell I in a $k \times k$ sized neighbourhood, for a histogram and calculate the entropy as follows (Holden *et al.* 2008, 2010):

$$E = -\sum_{i=1}^{n} P_i \log P_i, \tag{5}$$

where the histogram of n bins has been normalized to produce the probability P.

The standard deviation provides an approximation of the local data discrepancy. For each grid cell, the standard deviation of the nearby data values is determined. When compared to the background signal, significant features frequently show great fluctuation. For a window with N cells and a mean value of μ, the standard deviation σ of the cell values x_i is

$$\sigma = \sqrt{\frac{1}{N}\sum_{i=1}^{N}(x_i - \mu)^2}. \tag{6}$$

Source parameter imaging (SPI) typically generates the outputs of images from which depth to magnetic sources can be measured (Smith *et al.* 1998). According to Smith *et al.* (1998), this procedure examines the qualities of the second vertical derivative, and analytical signal responses. The analysis can provide a suitable geologic model, and unlike the standard Euler deconvolution (SED) (Smith *et al.* 1998), the depth estimate is non-reliant on any assumptions made on the geologic model. In addition, a reduction-to-pole filter does not need to be applied to the input grid because the approximated depth results are independent of the angle of declination and inclination of the magnetic field. When one has a thorough understanding of the local geology, magnetic data interpretation techniques become noticeably easier (Thurston and Smith 1997). The wavelength of the ASIG is typically where SPI approximations of depth come from. The ASIG based on Nabighian (1972), $A_1(x, z)$ is given as

$$A_1(x,z) = \frac{\partial M(x,z)}{\partial x} - j\frac{\partial M(x,z)}{\partial z}, \tag{7}$$

j is the imaginary number, x and z are Cartesian coordinates for the horizontal and the vertical directions perpendicular to the strike, respectively, and $M(x, z)$ is the magnitude of the anomalous total magnetic field.

The Euler homogeneity equation offers apparent depth to the magnetic sources. This procedure relates the magnetic field and its gradient components to the position of magnetic anomaly, with the degree of homogeneity defined as a 'structural index'. The Euler's homogeneity equation for magnetic data can be expressed as

$$(x - x_0)\frac{\partial T}{\partial x} + (y - y_0)\frac{\partial T}{\partial y}(z - z_0)\frac{\partial T}{\partial z} = N(B - T), \tag{8}$$

where (x_0, y_0, z_0) is the location of the magnetic body whose total field (T) is observed at (x, y, z). N, a measurement of the magnetic field fall-off rate, can be taken to be the structural index (SI), and B is the local magnetic field. The approach entails choosing a suitable SI value and resolving the equation for the best x_0, y_0, z_0, and B using least-square inversion. Additionally, a square window size that designates the number of gridded data cells to be employed in the inversion at each chosen solution must be supplied.

4. Results

The application of the CET method in this study enabled the generation of widespread subsurface geological structures, detailed mapping, and interpretation (Heal *et al.* 2014). The results of this research have enhanced the understanding of the complex structural pattern of the study area. Applying the CET grid analysis, favourable exploration targets can be mapped within the Precambrian Obudu Basement Complex or along lithological contacts between the OGS and the YGS (Nwankwo 2009, Ajibade *et al.* 2010). By using the CET

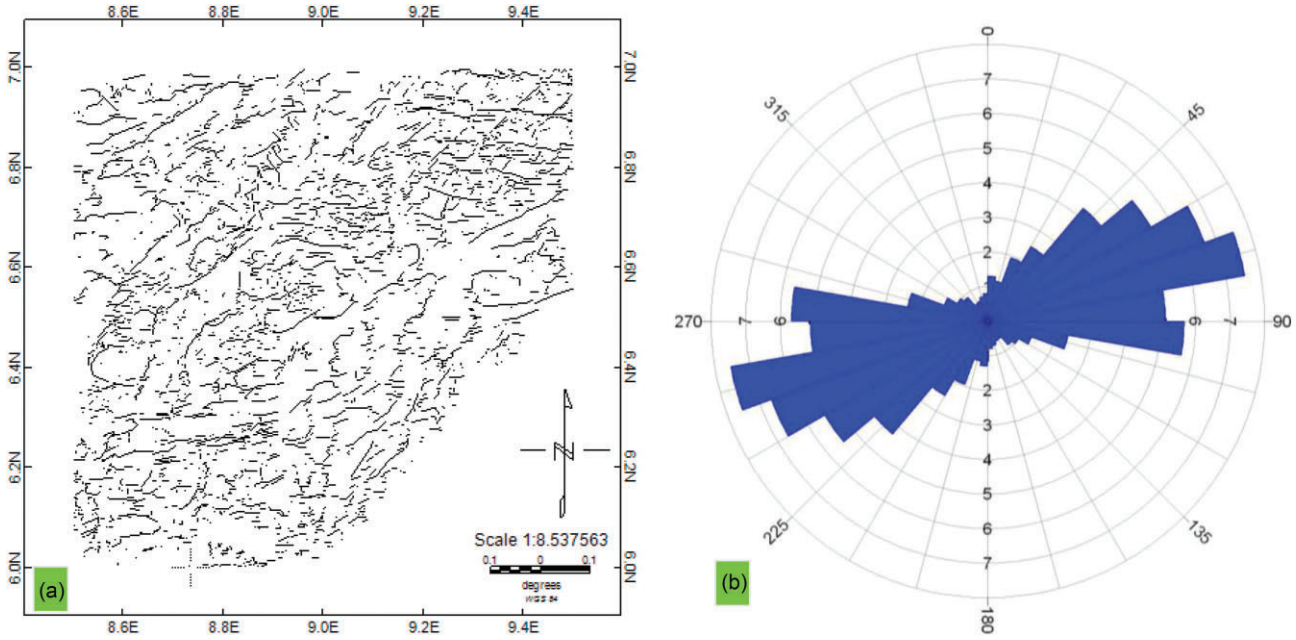

Figure 5. CET filter applied on total magnetic intensity data.

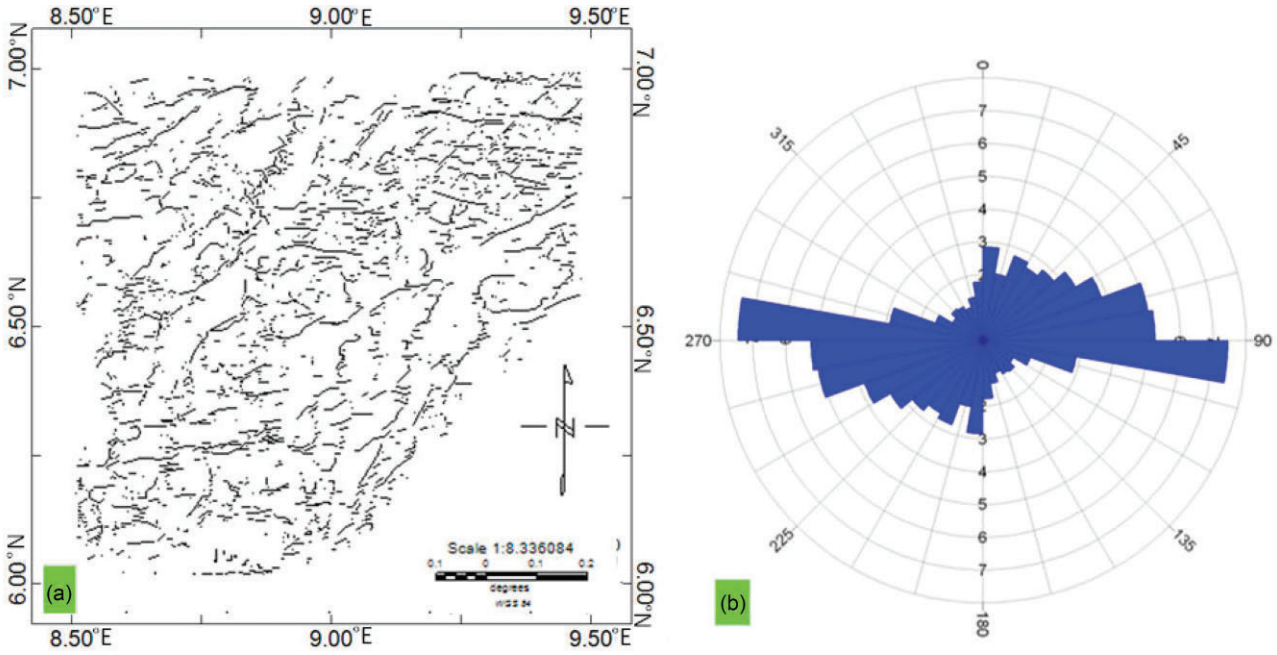

Figure 6. CET filter applied on first-vertical derivative gridded data.

approach on the TMI data, FVD, THD, TDR, and ASIG grids, these geologic features were examined. The analysis ultimately resulted in the construction of a detailed structural complexity map, which is very useful for mineral explorations.

The CET result obtained from the TMI data (Fig. 5) showed dominant NE–SW and minor E–W orientation of lineation. Figure 6 shows the result of the CET procedure applied on the FVD grid. The orientation of lineation within the same study area trend in mainly E–W and NE–SW orientations with minor N–S and NNE–SSW directions. These slight variations from the dominant NE–SW trend may be due to the enhancement of near-surface magnetic sources (Ekwok *et al.* 2020b; Reeves *et al.* 1997). Furthermore, the application of CET on THD (Fig. 7), TDR (Fig. 8), and ASIG (Fig. 9) show trends of N–S, NE–SW, NNE–SSW, and E–W orientations. In general, the predominant geologic structural orientation of NE–SW and NNE–SSW

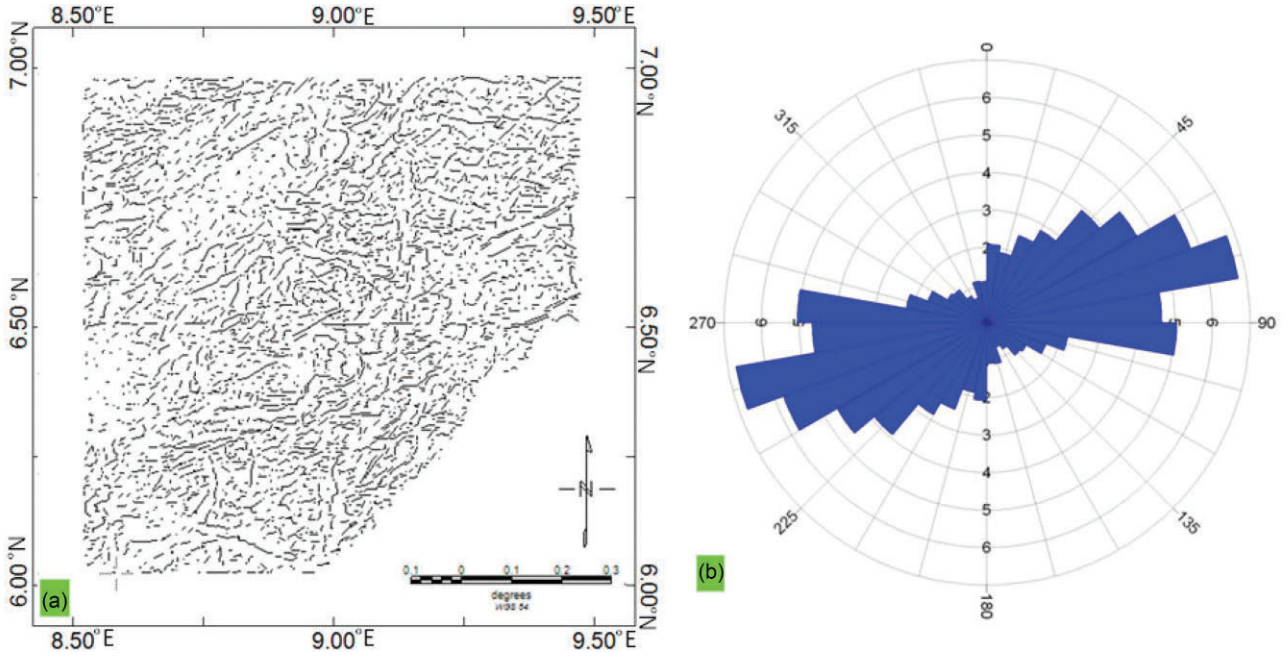

Figure 7. CET filter applied on THD gridded data.

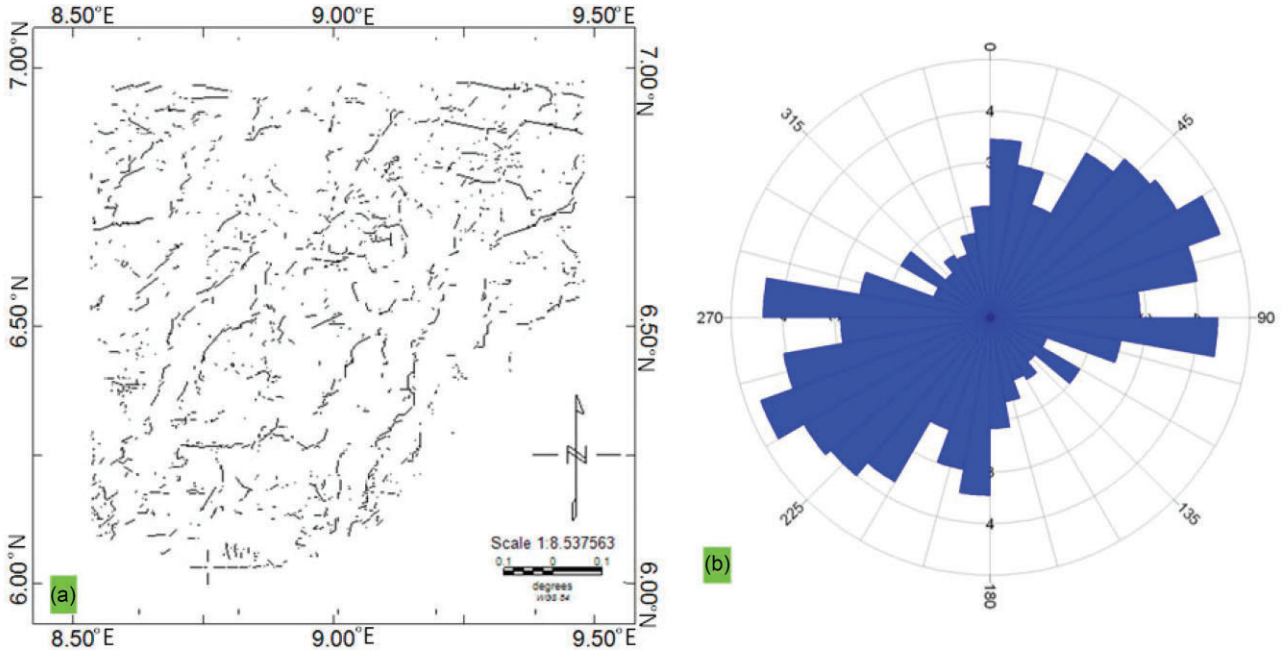

Figure 8. CET filter applied on tilt-angle derivative gridded data.

revealed by the rose petals represents the regional strike orientation. The principal strike orientation in the Lower Benue Trough and Obudu Basement Complex is represented by the rose petals in Figs. 5b, 6b, 7b, 8b, and 9b in the NE–SW and NNE–SSW. The Pan-African orogeny and subsequent post-orogenic events caused the NE and NNE lineaments to strike regionally (Nwankwo 2009, Ajibade *et al.* 2010). The complex pattern of the structural maps (Figs. 5a, 6a, 7a, 8a, and 9a) is a reflection of polyphase deformations caused by tectonic activity (Asouzu and Onyeagocha 2013). These deformations have formed various structural features, such as folds, faults, and shear zones, which have influenced the geometry of the rocks (Ajibade *et al.* 2010, Asouzu and Onyeagocha 2013).

To evaluate the depth solutions of these lineation in the Obudu Basement area, the SPI and SED (with SI = 1) were employed. Fig. 10 displays depth that varied from −76.6 to −583.3 m and indicated that the mapped structural features

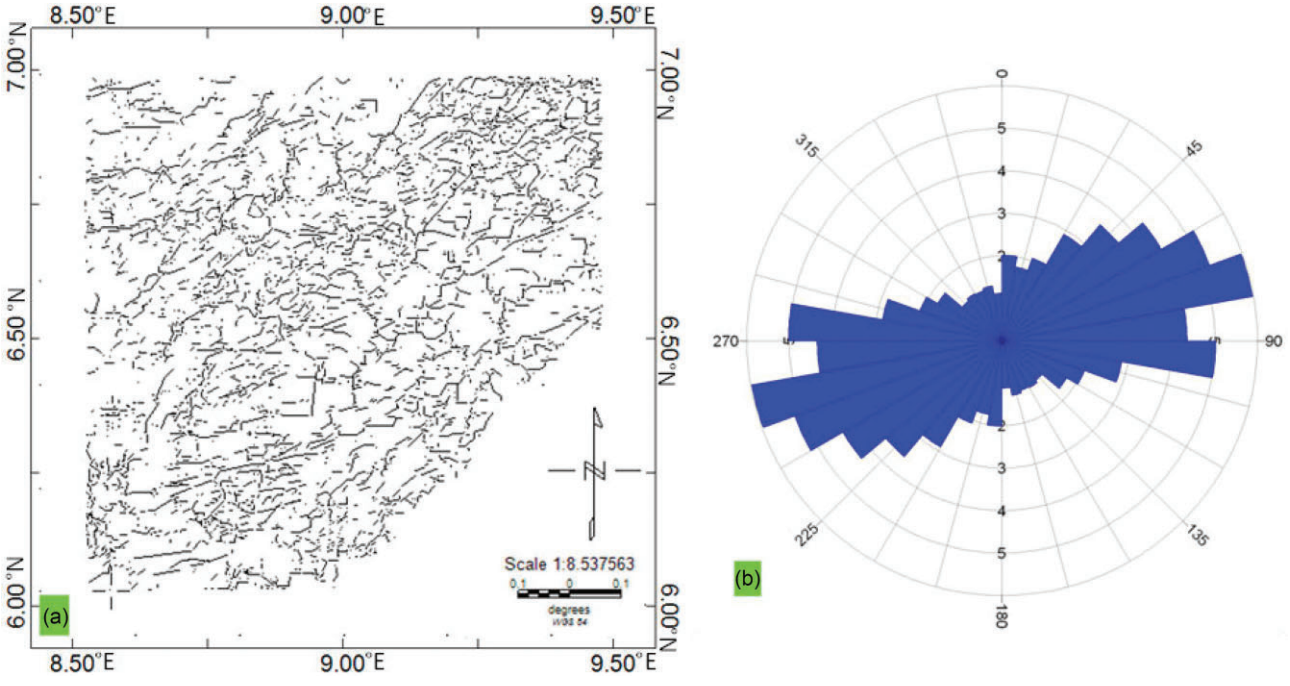

Figure 9. CET filter applied on ASIG gridded data.

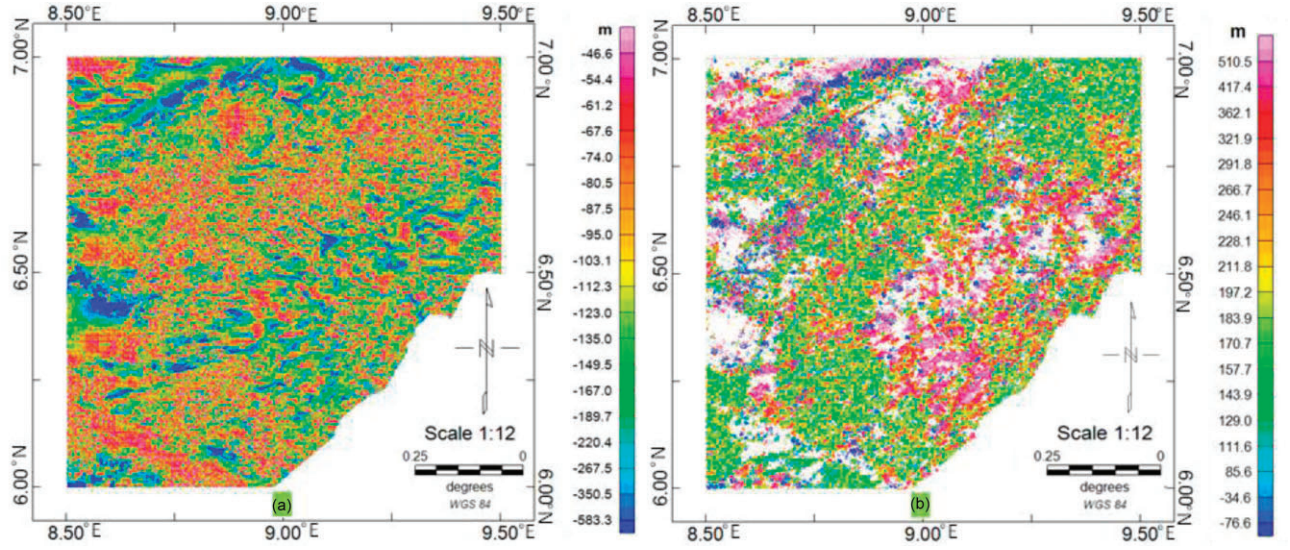

Figure 10. (a) SPI. (b) Euler deconvolution maps.

(Figs. 5b, 6b, 7b, 8b, and 9b) are shallowly placed not beyond 583.3 m. The results from earlier studies (Ekwok *et al.* 2021, Eldosouky *et al.* 2022a) are in agreement with these depth solutions. The SPI and conventional SED results display a wide range of colours that correspond to different basement depths in the research region. The SPI (Fig. 10a) indicates thin (pink-yellow), intermediate (yellow-lemon green), and thick (lemon green-blue) sedimentary cover of −46.6 to −95.0 m, −95.0 to −189.7 m, and −189.7 to −583.3 m, respectively. According to Thurston *et al.* (2000), the SPI map legend bar negative sign denotes a depth measurement that is downward from the Earth's surface. Likewise, the SED (Fig. 10b) displays depth variations of −76.6 to 129.0 m (blue-lemon green), 129.0 to 197.2 m (lemon green-yellow), and 197.2 to 510.5 m (yellow-pink) for thin, intermediate, and thick sedimentary covers, respectively. Areas characterized by thick sedimentation coincide with locations of deep valleys and depressions occupied by weathered materials from the elevated parts of the study area. Basement rocks with a cover were revealed in Fig. 10b with an estimated outcrop height of 76.6 m. In general, the investigated area is predominated by thin and highly weathered

sedimentary materials overlying complex structural features caused by Pan-African orogeny and successive post-orogenic events (Nwankwo 2009, Ajibade *et al.* 2010).

5. Discussion

A significant advancement in the CET involves the interpretation of magnetic results with geological and structural information (Uwiduhaye *et al.* 2021). Combining these datasets makes it possible to generate an in-depth understanding of the lineaments, leading to an increased probability of precisely identifying mineral and hydrothermal resource deposits (Ekwok *et al.* 2020, Uwiduhaye *et al.* 2021, Bencharef *et al.* 2022, Mahdi *et al.* 2022). These methods have resulted in the successful identification of geological structures that are viable for mineral exploration (Ekwok *et al.* 2021, 2022a; Kharbish *et al.* 2022, Abdelrahman *et al.* 2023b).

This investigation, which was carried out in the Precambrian Obudu Basement Complex, showed how well the CET grid analysis method works for deciphering and evaluating aeromagnetic data. The detection and interpretation of lineaments with different orientations, including the NE–SW, NNE–SSW, N–S, and E–W orientations, were made possible by this cutting-edge technique when it was applied to the processed and augmented aeromagnetic datasets (Figs. 5–9). Comparatively, from the observed CET results obtained from the various enhanced grids, note that Figs. 5 and 7–9 generated more reliable complex structural patterns, than Fig. 6. Generally, the leading geologic structural orientations of NE–SW and NNE–SSW, as characterized by the rose petals, reveal the regional strike orientation. The adjoining Cretaceous sediments of the Lower Benue Trough have been reported to be characterized by similar structural patterns (Ekwok *et al.* 2022a). The regional geologic study by Benkhelil (1987) revealed that the key structural configuration of the Obudu Basement Complex, Benue Trough, and Abakaliki Anticlinorium is in the NE–SW direction, while some E–W and N–S lineament orientations are regarded as transverse geologic structures to the predominant NE–SW and NNE–SSW fractures that serve as weak zones for massive invasion of the OGS (Asouzu and Onyeagocha 2013, Obiora *et al.* 2016) by granites, dolerites, and quartzo-feldspathic (Haruna 2017). The massive invasion of the OGS by the YGS resulted in a series of metamorphism (Nwankwo 2009), folds, faults, and shear zones (Ajibade *et al.* 2010, Asouzu and Onyeagocha 2013) with N–S, NNE–SSW, NW–SE, NE–WS, and E–W arrangements, reflecting the regional strike of lineaments associated with the Pan-African orogeny and succeeding post-orogenic events (Ajibade *et al.* 2010). The polyphase deformational history of the basement rocks reflects various occurrences of tectonic events (Asouzu and Onyeagocha 2013) that have influenced the geometry of the basement rocks (Ajibade *et al.* 2010, Asouzu and Onyeagocha 2013). According to reports, lineaments within tectonically active zones act as depositional structures for igneous-related minerals and migratory pathways for hydrothermal fluids (GSC 1992, Airo 2002, USGS 2013). Magmatism and mineralization are linked, according to several investigations (e.g. GSC 1992, Ekwok *et al.* 2020a; Airo 2002, Haruna 2017). Therefore, it is believed that vast quantities of metallogenic minerals in the studied area are under the influence of magmatic intrusions. The metallogeny of the Nigerian basement rocks (Orajaka 1973, Olade 1980, Woakes *et al.* 1987, Haruna 2017) have been investigated and properly documented. Ekwok *et al.* (2022a) reported that the study area is dominated by tectonothermal events, and these are characterized by long and short wavelength magnetic anomalies of geologic origin. Within the area, dense concentrations of short wavelength anomalies were reported to be caused by tectonisms (Ekwok *et al.* 2021), and these results agreed with the findings obtained by Oha *et al.* (2016). The adjoining Lower Benue Trough have been described by preceding researchers (Oha *et al.* 2016, Ekwok *et al.* 2020) to be hydrothermally altered and characterized by faults, fractures, fissures, dykes, sills, and baked Albian shales (Akpan *et al.* 2023). Within the southeast of Nigeria, various enhancement operations carried out on potential field data could be mapped to the N–S trending Santonian Abakaliki Anticlinorium (Benkhelil 1987, Oha *et al.* 2016), NE–SW dominant trend of lineaments (Ekwok *et al.* 2021, 2022a, 2020) Quaternary–Recent basaltic intrusions (Akpan *et al.* 2016, 2018), and the Precambrian Obudu Basement Complex has been reported to be rich in magnetite and intruded by dolerites, granites, and quartzo-feldspathic (Woakes *et al.* 1987, Haruna 2017, Agbi and Ekwueme 2018). The previously reported lineaments trend of the majorly NE–SW direction agrees with the key orientation of geologic structures reported this research. Conceivably, the intruded YGS extends to the upper mantle (Haruna 2017), which is possibly the source of hydrothermal fluids (that is, super enriched metalliferous brines) (USGS 2013, Mineral Resources of the Western US 2017).

The thin sedimentary cover (not exceeding 583.3 m) detected in the study location (which agrees with the finding of Ekwok *et al.* 2020a), is caused by the extensive occurrence of the basement in outcrop sections (Haruna 2017). The depth results (Fig. 10), which agree relatively well with each other, indicate regions of thick sedimentation (−189.7 to −583.3 m) that match with the positions of valleys and depressions filled with weathered materials. By contrast, depth estimations in the adjoining Lower Benue Trough were reported in the range of 2500 to 8000 m (Ofoegbu and Onuoha 1991, Uma 1998, Oha *et al.* 2016 etc.). Also, the depth to shallow sources within the southeast of Nigeria were earlier observed to be generally <600 m (Uma 1998,

Oha *et al.* 2016). The depth solutions (−189.7 to −583.3 m) obtained in this study correlate relatively well with previous findings (Uma 1998, Oha *et al.* 2016). Such areas with thin sedimentary sections were observed to coincide locations like the Obudu Basement Complex and the massively invaded Albian shales by the Santonian intrusions (Ofoegbu and Onuoha 1991, Uma 1998, Oha *et al.* 2016). Generally, the depth results from this study show that the geologic structures occur close the surface of the Earth.

6. Conclusion

This study demonstrates the use of the CET method to analyse magnetic intensity data and derive geologic structural orientations from the Obudu Basement Complex, Nigeria. The results highlight dominant NNE–SSW and NE–SW trends of lineation, along with minor N–S and E–W orientations within the study location. The slight deviation from the dominant NNE–SSW and NE–SW trends is attributed to the enhanced influence of near-surface igneous intrusions of the YGS of the post-orogenic events. Furthermore, the analysis of CET-derived structural maps from TMI, ASIG, FVD, THD, and TDR revealed comprehensive structural trends, further emphasizing the complex nature of the geologic structures. The main NNE–SSW and NE–SW orientations signify the major strike directions in the Precambrian Basement Complex, reflecting the regional strike of lineaments associated with the Pan-African orogeny and subsequent post-orogenic activities. These findings enhance our understanding of the structural evolution as well as geological processes within the investigated area. Furthermore, depth assessment involving SPI and SED methods revealed sediment coverage in the range of −76.6 to −583.3 m. Generally, the thin sedimentation (≤583.3 m) observed in the investigated location is a result of widespread basement outcrops. In general, these complex geologic structures occur as near-surface features, and they are potential sites for metallogenic minerals.

Acknowledgements

This research was supported by Researchers Supporting Project number (grant no. RSP2024R496), King Saud University, Riyadh, Saudi Arabia.

Conflict of interest statement

The authors declare no conflict of interest.

Data availability

The data underlying this article are available upon request from the corresponding author.

References

Abdelrahman K, Ekwok SE, Ulem CA *et al.* Exploratory mapping of the geothermal anomalies in the neoproterozoic Arabian Shield, Saudi Arabia, using magnetic data. *Minerals* 2023a;**13**:694. https://doi.org/10.3390/min13050694

Abdelrahman K, El-Qassas RAY, Fnais MS *et al.* Geological structures controlling Au/Ba mineralization from aeromagnetic data: Harrat ad Danun Area, Saudi Arabia. *Minerals* 2023b;**13**:866. https://doi.org/10.3390/min13070866

Agbi I, Ekwueme BN. Preliminary review of the geology of the hornblende biotite gneisses of Obudu Plateau Southeastern Nigeria. *Global J Geol Sci* 2018;**17**:75–83. https://doi.org/10.4314/gjgs.v17i1.7

Airo ML. Aeromagnetic and aeroradiometric response to hydrothermal alteration. *Surv Geophys* 2002;**23**:273–302. https://doi.org/10.1023/A:1015556614694

Ajibade AC, Oyawoye MO, Rahaman MA *et al.* Petrology of migmatites of the Obudu Plateau, Nigeria. *J Afr Earth Sci*. 2010;**56**:23–30.

Akpan AE, Ekwok SE, Ben UC *et al.* Direct detection of groundwater accumulation zones in Saprock Aquifers in tectono-thermal environments. *Water* 2023;**15**:3946. https://doi.org/10.3390/w15223946

Akpan AE, Ekwok SE, Ebong ED. Seasonal reversals in groundwater flow direction and its role in the recurrent Agwagune landslide problem: a geophysical and geological appraisal. *Environ Earth Sci*. 2016;**75**:1–17. https://doi.org/10.1007/s12665-015-5043-x

Akpan AE, Ekwok SE, Ebong ED *et al.* Coupled geophysical characterization of shallow fluvio-clastic sediments in Agwagune, southeastern Nigeria. *J Afr Earth Sci*. 2018;**143**:67–78. https://doi.org/10.1016/j.jafrearsci.2018.03.012

Alfaifi HJ, Ekwok SE, Ulem CA *et al.* Exploratory assessment of geothermal resources in some parts of the Middle Benue Trough of Nigeria using airborne potential field data. *J King Saud Univ Sci* 2023;**35**:102521. https://doi.org/10.1016/j.jksus.2022.102521

Asouzu EC, Onyeagocha AC. Geology and mineralization of the Obudu area of southeastern Nigeria. *J Afr Earth Sci* 2013;**86**:20–34.

Ben UC, Ekwok SE, Achadu OIM *et al.* A novel method for estimating model parameters from geophysical anomalies of structural faults using the Manta-Ray foraging optimization. *Front Earth Sci* 2022b;**10**:870299. https://doi.org/10.3389/feart.2022.870299

Ben UC, Ekwok SE, Akpan AE *et al.* Interpretation of magnetic anomalies by simple geometrical structures using the manta-ray foraging optimization. *Front Earth Sci* 2022a;**10**:849079. https://doi.org/10.3389/feart.2022.849079

Bencharef MH, Eldosouky AM, Zamzam S *et al.* Polymetallic mineralization prospectivity modelling using multi-geospatial data in logistic regression: the Diapiric Zone, Northeastern Algeria. *Geocarto Int* 2022;**37**:15392–427. https://doi.org/10.1080/10106049.2022.2097481

Benkhelil J. The origin and evolution of the cretaceous Benue Trough (Nigeria). *J African Earth Sci* 1987;**8**:251–82. https://doi.org/10.1016/S0899-5362(89)80028-4

Blakely RJ. *Potential Theory in Gravity and Magnetic Applications*. Cambridge University Press. 1996.

Cooper GRJ, Cowan DR. Enhancing potential field data using filters based on the local phase. *Comput Geosci* 2006;**32**:1585–91.

Davis K, Li Y. Enhancement of depth estimation techniques with amplitude analysis SEG. *Houston International Exposition and Annual Meeting* 2009.

Dentith MC, Mudge ST. *Geophysics for the Mineral Exploration Geoscientist.* Cambridge University Press. 2014.

Ekwok SE, Akpan AE, Achadu OIM *et al.* Structural and lithological interpretation of aero-geophysical data in parts of the Lower Benue Trough

and Obudu Plateau, Southeast Nigeria. *Adv Space Res* 2021;**68**:2841–54. https://doi.org/10.1016/j.asr.2021.05.019

Ekwok SE, Akpan AE, Kudamnya EA. Exploratory mapping of structures controlling mineralization in Southeast Nigeria using high resolution airborne magnetic data. *J Afr Earth Sci* 2020;**162**:103700. https://doi.org/10.1016/j.jafrearsci.2019.103700

Ekwok SE, Eldosouky AM, Achadu OIM *et al.* Application of the enhanced horizontal gradient amplitude (EHGA) filter in mapping of geological structures involving magnetic data in Southeast Nigeria. *J King Saud Univ Sci* 2022a;**34**:102288. https://doi.org/10.1016/j.jksus.2022.102288

Ekwok SE, Eldosouky AM, Ben UC *et al.* Application of high-precision filters on airborne magnetic data: a case study of the Ogoja tegion, Southeast Nigeria. *Minerals* 2022b;**12**:1227. https://doi.org/10.3390/min12101227

Ekwok SE, Eldosouky AM, Ben UC *et al.* An integrated approach of advanced methods for mapping geologic structures and sedimentary thickness in Ukelle and adjoining region (Southeast Nigeria). *Earth Sci Res J* 2023a;**27**:251–8. https://doi.org/10.15446/esrj.v27n3.105868

Ekwok SE, Eldosouky AM, Essa KS *et al.* Particle swarm optimization (PSO) of high-quality magnetic data of the Obudu Basement Complex, Nigeria. *Minerals* 2023b;**13**:1209. https://doi.org/10.3390/min13091209

Eldosouky AM, Ekwok SE, Akpan AE *et al.* Delineation of structural lineaments of Southeast Nigeria using high resolution aeromagnetic data. *Open Geosci* 2022a;**14**:331–40. https://doi.org/10.1515/geo-2022-0360

Eldosouky AM, Pham LT, Abdelrahman K *et al.* Mapping structural features of the Wadi Umm Dulfah area using aeromagnetic data. *J King Saud Univ Sci* 2022b;**34**:101803, ISSN 1018-3647, https://doi.org/10.1016/j.jksus.2021.101803

Elkhateeb SO, Eldosouky AM, Khalifa MO *et al.* Probability of mineral occurrence in the Southeast of Aswan area, Egypt, from the analysis of aeromagnetic data. *Arabian J Geosci* 2021;**14**:1514. https://doi.org/10.1007/s12517-021-07997-1

Fedi M, Florio G. Detection of potential fields source boundaries by enhanced horizontal derivative method. *Geophys Prospect* 2001;**49**:40–58. https://doi.org/10.1046/j.1365-2478.2001.00235.x

Geological Survey of Canada (GSC). *Airborne Geophysical Survey, Mount Milligan Area, British Columbia (NTS 93 O/4W, N/1, N/2E);* GSC Open File 2535. 1992.

Grose L, Pawley M, Czarnota K *et al.* Implicit modelling of structurally complex geological domains: an ore deposit case study from the Yilgarn Craton, Western Australia. *Ore Geol Rev* 2017;**81**:159–76.

Haruna IV. Review of the basement geology and mineral belts of Nigeria. *J Appl Geol Geophys* 2017;**5**:37–45.

Heal P, McCuaig TC, Harris LB. The Centre for Exploration Targeting: creating new paradigms for exploration targeting. *Aust J Earth Sci* 2014;**61**:635–40.

Holden E-J, Dentith M, Kovesi P. Towards the automatic analysis of regional aeromagnetic data to identify regions prospective for gold deposits. *Comput Geosci* 2008;**34**:1505–13.

Holden E-J, Kovesi P, Dentith M *et al.* Detection of regions of structural complexity within aeromagnetic data using image analysis. *Twenty Fifth International Conference of Image and Vision Computing New Zealand, 8–9 November 2010* 2010.

Jessell MW, Ailleres L, de Kemp EA *et al.* The role of structural geology in mineral exploration. *Nat Resour Res* 2016;**25**:279–95.

Kharbish S, Eldosouky AM, Amer O. Integrating mineralogy, geochemistry and aeromagnetic data for detecting Fe–Ti ore deposits bearing layered mafic intrusion, Akab El-Negum, Eastern Desert, Egypt. *Sci Rep* 2022;**12**:15474. https://doi.org/10.1038/s41598-022-19760-x

Kovesi K. Image features from phase congruency. *Videre: J Comput Vis Res* 1991; Summer, **1**. The MIT Press.

Kovesi P. Symmetry and asymmetry from local phase. AI'97. *Tenth Australian Joint Conference on Artificial Intelligence. 2–4 December 1997* 1997.

Kusky TM. *Geological Structures and Maps: A Practical Guide* 3rd edn. Springer. 2020.

Lam L, Lee S-W, Suen CY. Thinning methodologies–a comprehensive survey. *IEEE Trans Pattern Anal Mach Intell* 1992;**14**:879. https://doi.org/10.1109/34.161346

Mahdi AM, Eldosouky AM, El Khateeb SO *et al.* Integration of remote sensing and geophysical data for the extraction of hydrothermal alteration zones and lineaments; Gabal Shilman basement area, Southeastern Desert, Egypt. *J Afr Earth Sci* 2022;**194**:104640. https://doi.org/10.1016/j.jafrearsci.2022.104640

Miller HG, Singh V. Potential field tilt a new concept for location of potential field sources. *J Appl Geophys* 1994;**32**:213–7. https://doi.org/10.1016/0926-9851(94)90022-1

Milligan P, Gunn P. Enhancement and presentation of airborne geophysical data. *AGSO J Aust Geol Geophys* 1997;**17**:63–75.

Mineral resources of the western US. *The Teacher-Friendly Guide to the Earth Scientist of the Western US.* http://geology. Teacher friendly guide. Org /index. php/ mineral-w. 2017.

Nabighian MN. The analytical signal of two dimensional magnetic bodies with polygon cross-section: its properties and use for automated anomaly interpretation. *Geophysics* 1972;**37**:507–17. https://doi.org/10.1190/1.1440276

Nabighian MN. Towards the three-dimensional automatic interpretation of potential field data via generalized Hilbert transforms. Fundamental relations. *Geophysics* 1984;**53**:957–66.

Nabighian MN, Grauch VJS, Hansen RO *et al.* The historical development of the magnetic method in exploration. *Geophysics* 2005;**70**:33ND–61ND. https://doi.org/10.1190/1.2133784

Nwankwo LI. Structural styles in the Precambrian Basement Complex of southeastern Nigeria. *J Afr Earth Sci* 2009;**53**:73–86.

Obiora DN, Igwe EO, Nwachukwu SO. Petrology and structural evolution of the high-grade terrain around Obudu and Oban massifs, southeastern Nigeria. *J Afr Earth Sci* 2016;**117**:42–58.

Ofoegbu CO, Onuoha KM. Analysis of magnetic data over the Abakaliki Anticlinolium of the Lower Benue Trough, Nigeria. *Mar Pet Geol* 1991;**8**:174–83. https://doi.org/10.1016/0264-8172(91)90005-L

Oha IA, Onuoha KM, Nwegbu AN *et al.* Interpretation of high resolution aeromagnetic data over southern Benue Trough, southeastern Nigeria. *J Earth Syst Sci* 2016;**125**:369–85. https://doi.org/10.1007/s12040-016-0666-1

Olade MA. *Precambrian metallogeny in West Africa. Geol Rundsch* 1980;**69**:411–28. https://doi.org/10.1007/BF02104546

Orajaka SO. Possible metallogenic provinces in Nigeria. *Econ Geol* 1973;**68**:278–80. https://doi.org/10.2113/gsecongeo.68.2.278

Pal SK, Majumdar TJ. Geological appraisal over the Singhbhum-Orissa Craton, India using GOCE, EIGEN6-C2 and in situ gravity data. *Int J Appl Earth Obs Geoinf* 2015;**11**:155–66.

Pham LT, Kafadar O, Oksum E *et al.* An improved approach for detecting the locations of the maxima in interpreting potential field data. *Arabian J Geosci* 2021a;**14**:43. https://doi.org/10.1007/s12517-020-06399-z

Pham LT, Nguyen DA, Eldosouky AM *et al.* Subsurface structural mapping from high- resolution gravity data using advanced processing methods. *J King Saud Univ Sci* 2021b;**33**:101488: ISSN 1018-3647, https://doi.org/10.1016/j.jksus.2021.101488

Prasad KND, Pham LT, Singh AP. Structural mapping of potential field sources using BHG filter. *Geocarto Int* 2022;1–28. https://doi.org/10.1080/10106049.2022.2048903.

Reeves C, Reford S, Millingan P. Airborne geophysics: old methods, new images. In: Gubins A. (ed.), *Proceedings of the Fourth Decennial International Conference on Mineral Exploration*, 1997; 13–30 (Australia).

Reid AB, Allsop JM, Granser H *et al.* Magnetic interpretation in three dimensions using Euler deconvolution. *Geophysics* 1990;**55**:80–91. https://doi.org/10.1190/1.1442774

Richter C. *Seismic reflection and refraction surveys.* In *Encyclopedia of Engineering Geology* 2017; pp. 1–9. Springer.

Roest WR, Verhoef J, Pilkington M. Magnetic interpretation using the 3-D analytic signal. *Geophysics* 1992;**57**:116–25. https://doi.org/10.1190/1.1443174

Salem A, Ravat D. A combined analytic signal and Euler method (AN-EUL) for automatic interpretation of magnetic data. *Geophysics* 2003;**68**:1952–61. https://doi.org/10.1190/1.1635049

Salem A, Williams S, Fairhead JD *et al.* Tilt-depth method: a simple depth estimation method using first-order magnetic derivatives. *Leading Edge* 2007;**26**:1502–5. https://doi.org/10.1190/1.2821934

Smith J, Brown C, Blackwell M *et al.* Application of CET tools to mapping geological structures in challenging terrain. *J Appl Geophys* 2019;**161**:132–44.

Smith RS, Burgess S, Hickman S. *Fault-Related Rocks: a Photographic Atlas.* John Wiley & Sons. 2018.

Smith RS, Thurston JB, Dai T *et al.* iSPI™ the improved source parameter imaging method[1]. *Geophys Prospect* 1998;**46**:141–51. https://doi.org/10.1046/j.1365-2478.1998.00084.x

Thompson DT, Shearer PM, Arkani-Hamed J. Enhanced Euler deconvolution with a priori dip constraints for the interpretation of magnetic data. *Geophysics* 2019;**84**:J1–J13.

Thurston JB, Smith RS. Automatic conversion of magnetic data to depth, dip, and susceptibility contrast using SPI™ method. *Geophysics* 1997;**62**:807–13. https://doi.org/10.1190/1.1444190

Thurston JB, Smith RS, Guillon JC. A multi-model method for depth estimation from magnetic data. *Geophysics* 2000;**67**:555–61. https://doi.org/10.1190/1.1468616

Tselentis GA, Raptakis DG, Papadimitriou P *et al. Field surveying methods for engineering geological mapping.* In *Engineering Geological Advances in Geotechnical Infrastructure and Monitoring* 2020; pp. 3–33. Springer.

Uma KO. The brine fields of the Benue Trough, Nigeria: a comparative study of geomorphic, tectonic and hydrochemical properties. *J Afr Earth Sci* 1998;**26**:261–75. https://doi.org/10.1016/S0899-5362(98)00009-8

United States Geological Survey (USGS). *Setting and Origin of Iron Oxide-copper- cobalt-gold-rare Earth Element Deposits of Southeast Missouri*: 2013; http://minerals.usgs.gov/east/semissouri/index.html

Uwiduhaye JD, Ngaruye JC, Saibi H. Defining potential mineral exploration from the interpretation of aeromagnetic data in Western Rwanda. *Ore Geol Rev* 2021;**128**:103927. https://doi.org/10.1016/j.oregeorev.2020.103927

Wijns C, Perez C, Kowalczyk P. Theta map: edge detection in magnetic data. *Geophysics* 2005;**70**:L39–43. https://doi.org/10.1190/1.1988184

Woakes M, Rahaman MA, Ajibade AC. Some metallogenetic features of the Nigerian basement. *J Afr Earth Sci* 1987;**6**:655–64.